Defect-Free Synthesis of a Fully π-Conjugated Helical Ladder Polymer and Resolution into a Pair of Enantiomeric Helical Ladders

Tomoyuki Ikai,*[a],[b] Sayaka Miyoshi,[a] Kosuke Oki,[a] Ranajit Saha,[c] Yuh Hijikata,[c] and Eiji Yashima*[a]

[a] Dr. T. Ikai, S. Miyoshi, Dr. K. Oki, Prof. E. Yashima
Department of Molecular and Macromolecular Chemistry
Graduate School of Engineering, Nagoya University
Chikusa-ku, Nagoya 464-8603 (Japan)
E-mail: ikai@chembio.nagoya-u.ac.jp; yashima@chembio.nagoya-u.ac.jp
[b] Dr. T. Ikai
Precursory Research for Embryonic Science and Technology (PRESTO)
Japan Science and Technology Agency (JST)
Kawaguchi, Saitama 332-0012 (Japan)
[c] Dr. R. Saha, Dr. Y. Hijikata
Institute for Chemical Reaction Design and Discovery (WPI-ICReDD)
Hokkaido University
Sapporo 001-0021 (Japan)

Supporting information for this article is given via a link at the end of the document.

Abstract: Fully π-conjugated ladder polymers with a spiral geometry represent a new class of helical polymers with great potential for organic nanodevices, but there is no precedent for an optically-active helical ladder polymer totally composed of achiral units. We now report the defect-free synthesis and resolution of a fully π-conjugated helical ladder polymer with a rigid helical cavity, which has been achieved by quantitative and chemoselective acid-promoted alkyne benzannulations of a rationally designed, random-coil achiral polymer followed by chromatographic enantioseparation. Because of a sufficiently high helix-inversion barrier, the isolated excess one-handed helical ladder polymer with the degree of polymerization of more than 15 showed a strong circular dichroism with the dissymmetry factor of up to 1.7×10^{-2} and is thermally stable, maintaining its optical activity in solution even at 100 °C, as well supported by molecular dynamics simulation.

Conjugated ladder polymers with a well-defined rigid coplanar backbone have been of tremendous interest due to their unique optical, electronic, and photophysical properties[1] since the first synthesis reported by Scherf and Müllen.[2] However, defect-free fully π-conjugated ladder polymers consisting of consecutively fused aromatic rings remain a synthetic challenge. Using the state-of-the-art synthetic technology, fully π-conjugated ladder polymers have been developed for use in organic electronic and optoelectronic devices,[3] such as photovoltaic cells,[4] field-effect transistors,[5] light emitting diodes,[6] capacitors,[7] actuators,[8] and thermoelectrics,[9] but their three-dimensional (3D) structures are characterized as linear ribbon or zigzag coplanar structures.[10] A limited number of fully π-conjugated ladder-like helical graphene nanoribbons has also been prepared with great interest[11] because of their potential use for a metal-free nanosolenoid,[11e] carbon nanotube dispersion,[11b] fluorescence sensing of explosives,[11d] and mechanical nanosprings showing a reversible metal-semiconductor transition.[12] However, all the previously reported coiled-shaped fully π-conjugated helical ladder polymers are racemic with no information about their helix stability. In addition, there is no precedent for fully π-conjugated helical ladders consisting of totally achiral repeating units showing an optical activity solely due to their macromolecular helicity.[13] Recently, Nuckolls and coworkers reported unique single-handed fully π-conjugated helical ladder polymers (helicene nanoribbons), which were, however, achieved by using a configurationally stable right (*P*)- or left (*M*)-handed-[6]helicene as the chiral framework.[14]

We recently succeeded in the defect-free synthesis of "partially conjugated" one-handed helical (poly-**A**,[15] poly-**B**,[16] and poly-**C**[17]) (Figure 1a) and "fully π-conjugated" achiral zigzag coplanar ladder polymers.[17] The overall 3D ladder geometry can be controlled by a combination of chiral/achiral (Figure 1a) and achiral/achiral comonomer units of the random-coil precursor polymers containing the same achiral 2,5-diethynyl-substituted *p*-phenylene segments, followed by acid-promoted intramolecular alkyne benzannulations. The helical handedness ((*P*)- or (*M*)-helix) and helical pitch (contracted or extended helix) of the helical ladder polymers are determined by the enantiopure 2,6-linked-triptycene and 6,6´- and 4,4´-linked-1,1´-spirobiindane units (Figure 1a). The quantitative[18] and chemoselective[16-17] acid-promoted alkyne benzannulations of the precursor polymers are of key importance, which relies on the 2,6-dimethyl substituents introduced on the phenylethynyl pendant groups[16-17] except for the bulky triptycene-bound poly-**A**.[15]

Here, we show that a rationally designed precursor polymer composed of alternating achiral 2,7-linked-fluorene and 2,4-diethynyl-substituted C_{2v}-symmetric *m*-phenylene units is quantitatively and chemoselectively converted into a fully π-conjugated ladder polymer with a spiral geometry through the acid-promoted annulative π-extension (Figure 1b). The racemic helical ladder polymer entirely consisting of achiral repeating units was, for the first time, separated into enantiomeric helices by chiral high-performance liquid chromatography (HPLC) (Figure 1c), which are stable even at 100 °C. The structure, dynamics, and stability of the helicity of the fully π-conjugated helical ladder polymer were also investigated by molecular dynamics (MD) simulation.

We first investigated the substituent effect of the 4-alkoxyphenyl pendants (H or 2,6-dimethyl; see Figure 1a (**R**[1] and

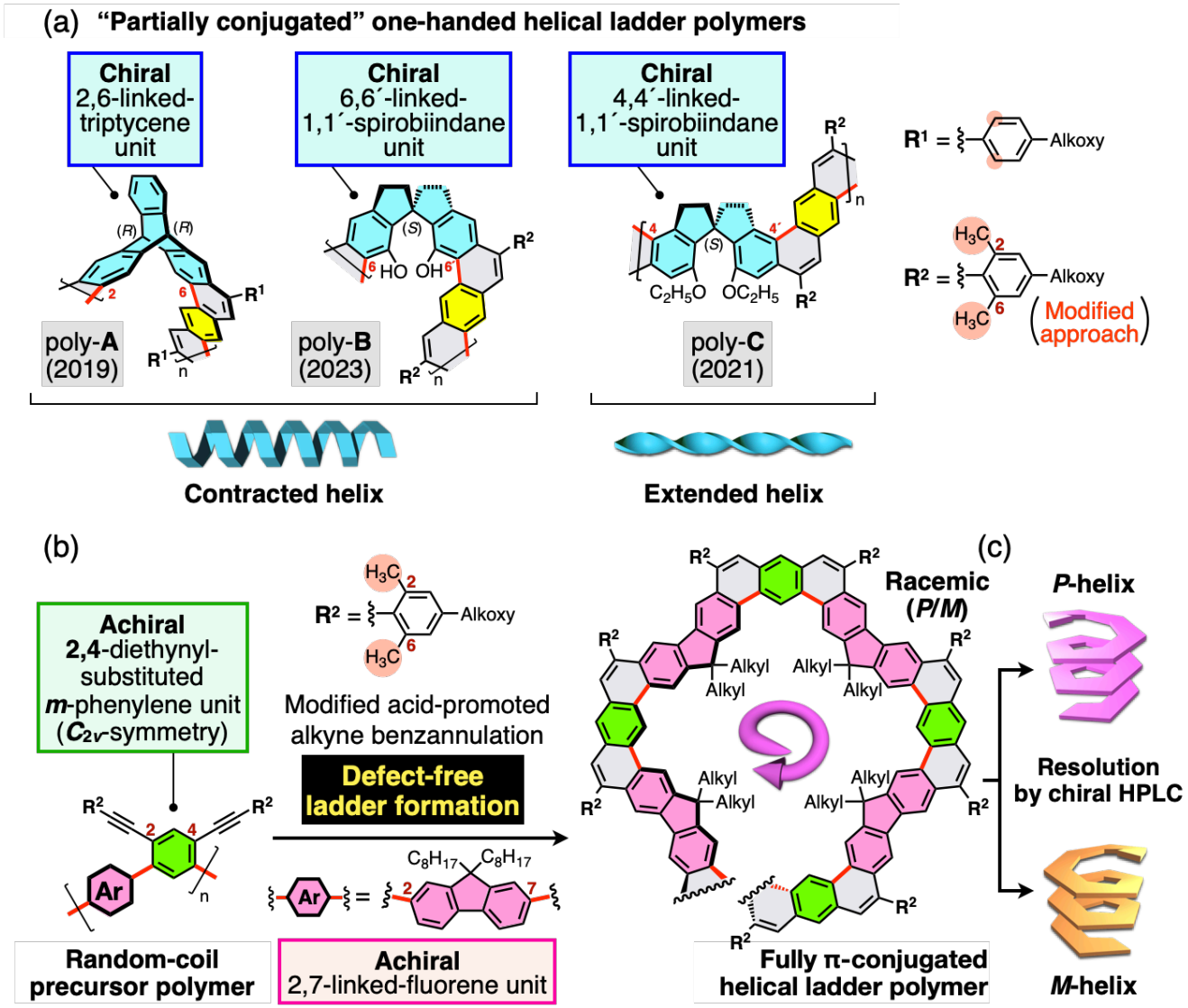

Figure 1. (a) Structures of the "partially conjugated" one-handed helical ladder polymers with contracted (poly-**A** and poly-**B**) and extended (poly-**C**) helical geometries containing enantiopure 2,6-linked-triptycene and 6,6´- and 4,4´-linked-1,1´-spirobiindane units, respectively. (b) Schematic illustrations of the defect-free synthesis of a fully π-conjugated helical ladder polymer through quantitative and chemoselective acid-promoted alkyne benzannulations of the corresponding random-coil precursor polymer composed of the achiral 2,4-diethynyl-substituted *m*-phenylene unit with C_{2v}-symmetry. (c) Enantioseparation of the racemic helical ladder polymer into right (*P*)- and left (*M*)-handed helical ladders by chiral HPLC.

R²)) on the trifluoroacetic acid (TFA)-promoted alkyne benzannulation using four kinds of fluorene (**1Me** and **1H**)- and *m*-phenylene (**3Me** and **3H**)-based cyclization model precursors (Schemes S1 and S2 and Figures 2, S1, and S2). The four- and two-fold intramolecular cyclizations of **1Me** and **3Me** completely proceeded without any side reactions, thus quantitatively and regioselectively producing **2Me** and **4Me**, respectively, as confirmed by their simple ^{1}H NMR spectra (Figure 2b(ii,iv)) as well as the 2D NMR (Figures S5 and S7) and IR analyses (Figure S3a,b,e,f). The fully π-conjugated fluorene-based ladder structure of **2Me** was unambiguously determined by single-crystal X-ray crystallography (Figure 2c), indicating that the cyclization reactions regioselectively occur at the 3- and 6-positions of the fluorene unit (Figure 2a).[17] The crystal packing structure revealed that **2Me** possesses a doubly twisted π-conjugated helical framework consisting of enantiomeric (*P*,*P*)- and (*M*,*M*)-**2Me** pairs, which are present in the unit cell (Figure 2d). In sharp contrast, the TFA-promoted alkyne benzannulations of **1H** (Figure S1) and **3H** (Figure S2) without the 2,6-dimethyl substituents gave three products, **2H-a**/**2H-b**/**2H-c** (46/45/9) and **4H-a**/**4H-b**/**4H-c** (59/33/8), respectively. These structural isomers were most likely produced by intramolecular multicyclizations with or without aryl migration (Figure S16)[17,19] and were fully characterized and identified by the high-resolution mass and 2D NMR analyses (Figures S9–S11 and S13–S15).

Based on the successful synthesis of the desired ladder models of **2Me** and **4Me**, we then synthesized a random-coil precursor polymer, poly-**7Me**, composed of alternating achiral 2,7-fluorene and 2,4-diethynyl-substituted *m*-phenylene units by the Suzuki–Miyaura coupling copolymerization of **5Me** and **6** (Figure 3a and Scheme S3). The number-average molar mass (M_n) and molar-mass dispersity (M_w/M_n) of the resulting poly-**7Me** after size-exclusion chromatography (SEC) fractionation were determined to be 4.96×10^4 and 2.64, respectively, which corresponds to the number-average degree of polymerization (DP_n) of 49.3 (Table S1). Poly-**7Me** was then subjected to the TFA-promoted alkyne

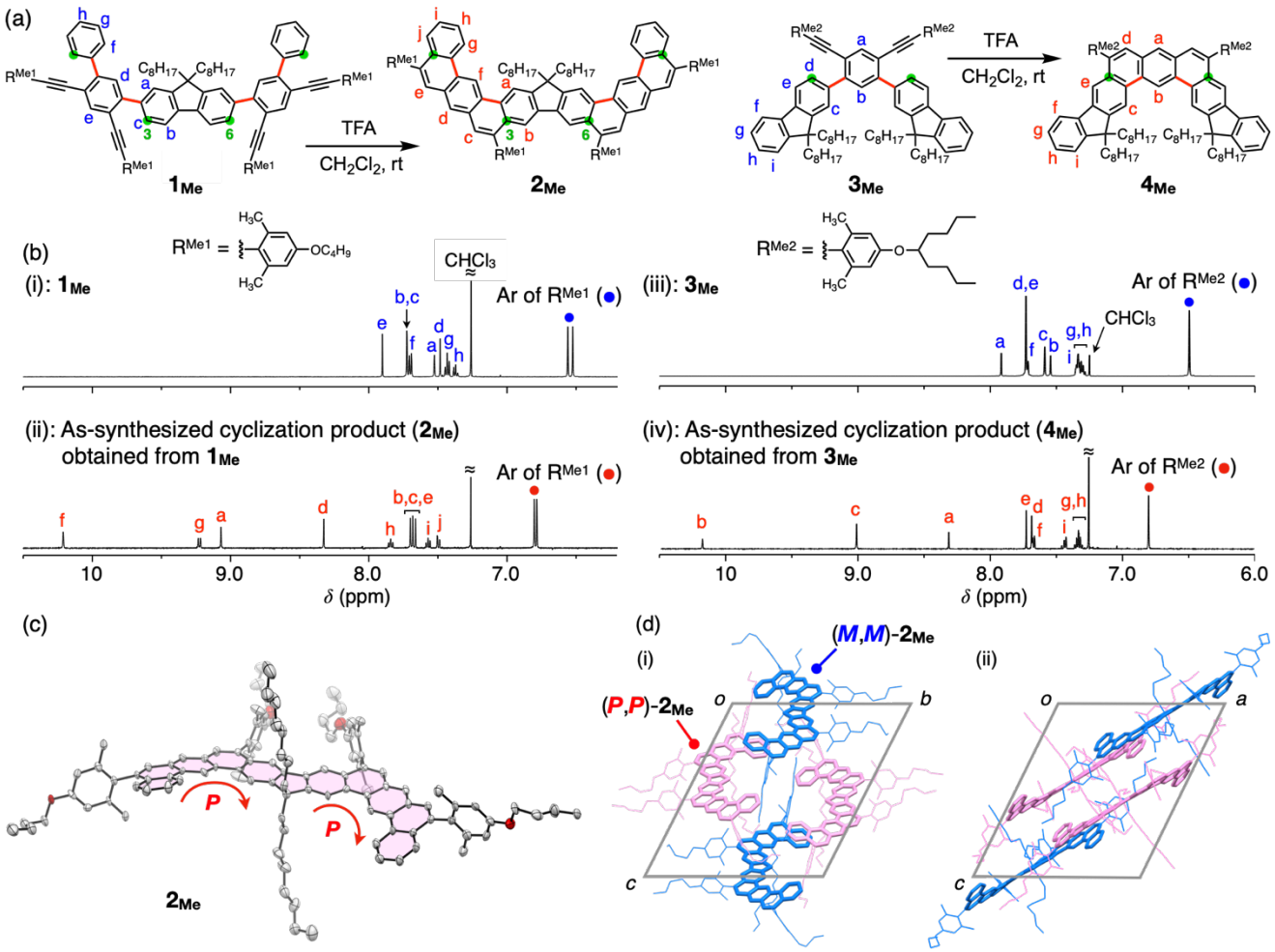

Figure 2. (a) Synthesis of fluorene-based fully π-conjugated ladder-type molecules (**2Me** and **4Me**) through acid-promoted alkyne benzannulations of their precursors (**1Me** and **3Me**). (b) ^{1}H NMR spectra (500 MHz, $CDCl_3$, 25 °C) of **1Me** (i) and **3Me** (iii) and the as-synthesized cyclization products (**2Me** (ii) and **4Me** (iv)) obtained from **1Me** and **3Me**, respectively. For the signal assignments and the corresponding IR spectra, see Figures S3–S7. (c) Perspective view of the crystal structure of **2Me** with thermal ellipsoids at 50% probability. (d) Crystal packing structure of (*P*,*P*)/(*M*,*M*)-**2Me** as viewed along the *a* (i) and *b* (ii) axes of the unit cell shown in gray. The fully π-conjugated ladder-type backbones and the 4-butoxy-2,6-dimethylphenyl pendant groups are represented by capped-stick and wireframe models, respectively, and (*P*,*P*)/(*M*,*M*)-**2Me** are colored in pink and blue, respectively. All the hydrogen atoms and disordered atoms are omitted for clarity.

benzannulation, which was completed within 6 h (Figure S3(i,j)), thus producing a defect-free fully π-conjugated ladder polymer, poly-**8Me** (Figure 3a), as supported by the matrix-assisted laser desorption-ionization time-of-flight mass analysis (Figure S17). The M_n (3.25×10^4) value of poly-**8Me** decreased to approximately two-thirds that of the precursor poly-**7Me** (Figure 3a and Scheme S4), probably due to the strictly limited conformational freedom of the ladder-type backbone as well as the compact and contracted helix formation, while mostly maintaining the dispersity (M_w/M_n = 2.72), as observed for the synthesis of the previously reported coiled-shaped helical ladder polymer.[15]

The ^{1}H NMR spectrum of poly-**8Me** (Figure 3b(ii)) exhibited a broad, but characteristic set of proton resonances, which could be unequivocally assigned by the 2D NMR analysis (Figures S18 and S19). The chemical shifts of the aromatic proton signals (H_a – H_e) of poly-**8Me** were reasonably consistent with those of the unit models (**2Me** and **4Me**) (Figure 2b(ii,iv)), thus supporting its regular ladder structure. As anticipated, when poly-**7H** lacking the 2,6-dimethyl substituents was treated with TFA, the ^{1}H NMR spectrum of the resulting poly-**8H** was rather complicated with minor broad peaks (e.g., around 8.0 and 9.5 ppm) because of its irregular backbone structure consisting of different repeating units (Figure S20) as revealed by its model reaction products (**2H-a–c** and **4H-a–c**) (Figures S1 and S2).

Interestingly, some of the main-chain aromatic protons (H_a, H_d, and H_e) of poly-**8Me** slightly shifted upfield when compared to those of poly-**8H** (Figure S20b(ii,iii)) and further split into two sets of signals of approximately equal intensity. The observed upfield shifts can be ascribed to its expanded helical ladder structure, in which the fully π-conjugated ladder polymer backbone is forced to fold into either a (*P*)- or (*M*)-handed, intramolecularly stacked helical conformation due to the *m*-phenylene skeleton of its precursor polymer, thus causing the ring current shielding effect. In fact, the MD simulation of an energy minimized (*M*)-handed helical ladder structure of poly-**8Me** (Figure 3d and Section 4 in the Supporting Information) revealed that poly-**8Me** possesses a spiral-shaped π-conjugated single-handed 4_1 helical backbone with the helical pitch (d_1 – d_3) of ca. 1.5 nm (Figure 3d), which is not constant but fluctuates in the range of ca. 1.0 nm over time along with a unique springlike extension/contraction motion (Figure 3e and Video S1),[20] and the helix diameter of ca. 2.5 nm, carrying all of the aryl pendants (R^{Me2}) at the periphery. Such a spiral-shaped helical backbone with a rigid helical cavity, in which the two octyl chains at the fluorene units are densely packed

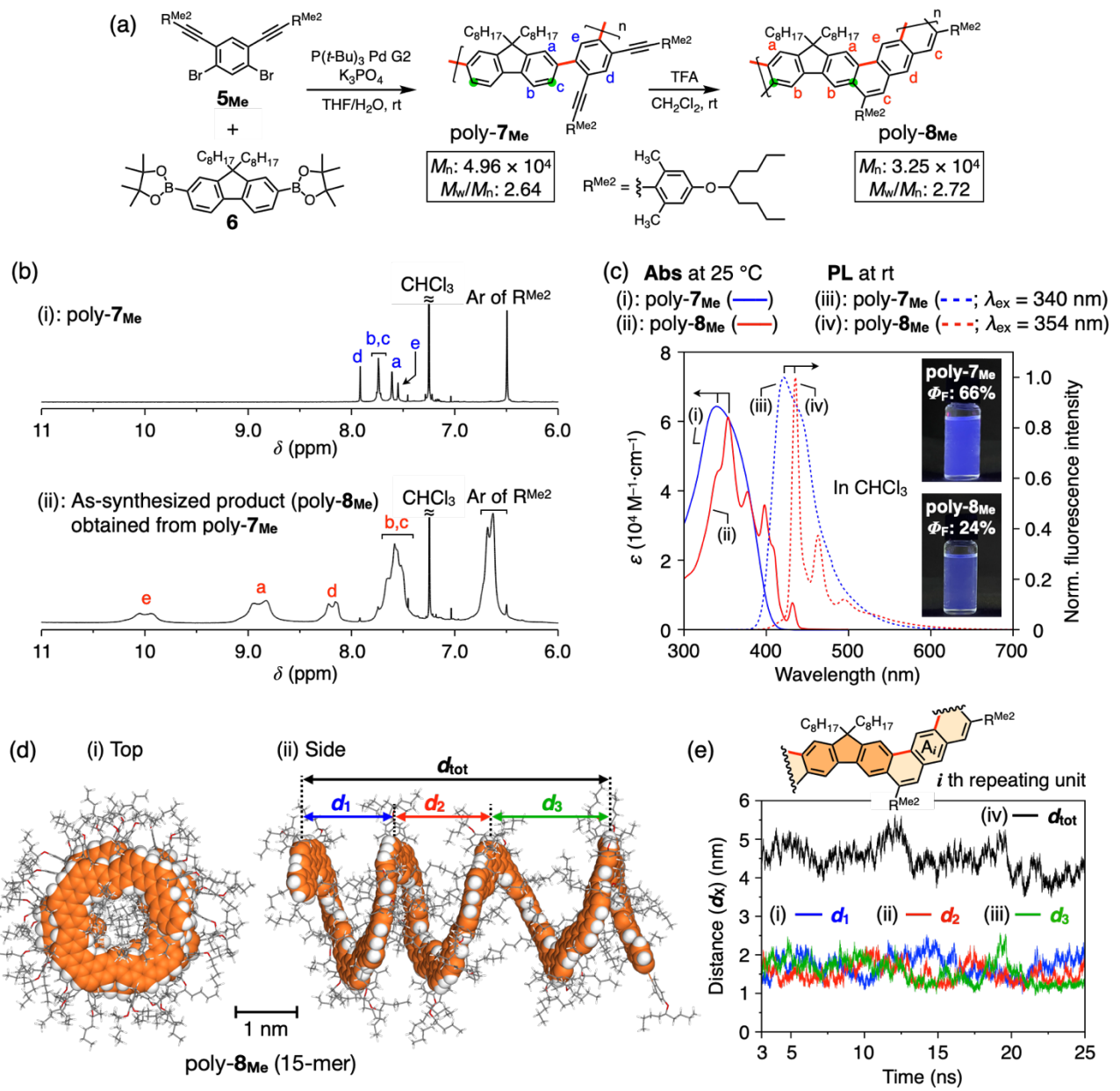

Figure 3. (a) Synthesis of a fully π-conjugated helical ladder polymer (poly-**8Me**) by the Suzuki–Miyaura coupling copolymerization of **5Me** and **6**, followed by quantitative and chemoselective alkyne benzannulations of poly-**7Me**. (b) ^{1}H NMR spectra (500 MHz, $CDCl_3$, 50 °C) of poly-**7Me** (i) and poly-**8Me** (ii). For the signal assignments, see Figures S18 and S19, respectively. (c) Absorption (solid lines) and normalized PL (dotted lines) spectra of poly-**7Me** (i,iii) and poly-**8Me** (ii,iv) in chloroform at 25 °C and room temperature, respectively. The insets show photographs of poly-**7Me** and poly-**8Me** in chloroform under irradiation at 365 nm. Fluorescence quantum yields (Φ_F) are also shown. [Repeating units of polymer] = 1.0 × 10^{-5} M. (d) Top (i) and side (ii) views of a model structure of the (*M*)-handed 4_1 helical poly-**8Me** with 15 repeating units. The snapshot at 3 ns during the MD simulation at 323 K (50 °C) is depicted. The carbon atoms of the helical ladder backbone are highlighted in orange. (e) Plots of the helical pitch lengths (d_1 (i), d_2 (ii), and d_3 (iii)) and the distance of three turns of the helix (d_{tot} (iv)), which are defined as distances between the centroids of the ring A_i in the [2nd and 6th], [6th and 10th], [10th and 14th], and [2nd and 14th] repeating units of the poly-**8Me** model, respectively (see Figure S23), during the MD simulation. The systems seemed to be equilibrated within the first 3 ns (see Figure S24), hence, the plots are shown from 3.0 to 25.0 ns.

(Figure 3d and Video S1), may cause splitting of the aromatic protons (H_a, H_d, and H_e) of poly-**8Me** (Figure 3b(ii)) due to atropisomers of the octyl chains generated by the highly-conformational restriction of the octyl chains.[21]

Further significant differences between poly-**8H** and poly-**8Me** as well as between poly-**8Me** and its precursor polymer (poly-**7Me**) were observed in their absorption and photoluminescence (PL) spectra (Figures 3c and S25). The defect-free helically stacked poly-**8Me** exhibited remarkably sharp and better resolved absorption and PL spectra than poly-**8H** with an irregular backbone structure because of its limited conformational freedom ((ii and iv) in Figures 3c and S25). On the other hand, the absorption and PL spectra of the random-coil precursor polymers (poly-**7Me** and poly-**7H**) were quite broad ((i and iii) in Figures 3c and S25). These absorption and PL spectral changes before and after ladderization are in good agreement with those of the unit models (Figures S26–S28).

To gain concrete evidence for the helical ladder structure of poly-**8Me** composed of achiral repeating units, we attempted the direct enantioseparation of the as-synthesized racemic helical poly-**8Me** by chiral HPLC using a series of chiral columns (Daicel, Osaka, Japan) under various eluent conditions (Figure 1c), although successful examples of the separation of racemic helical polymers into each helix are quite rare.[22] When poly-**8Me** was

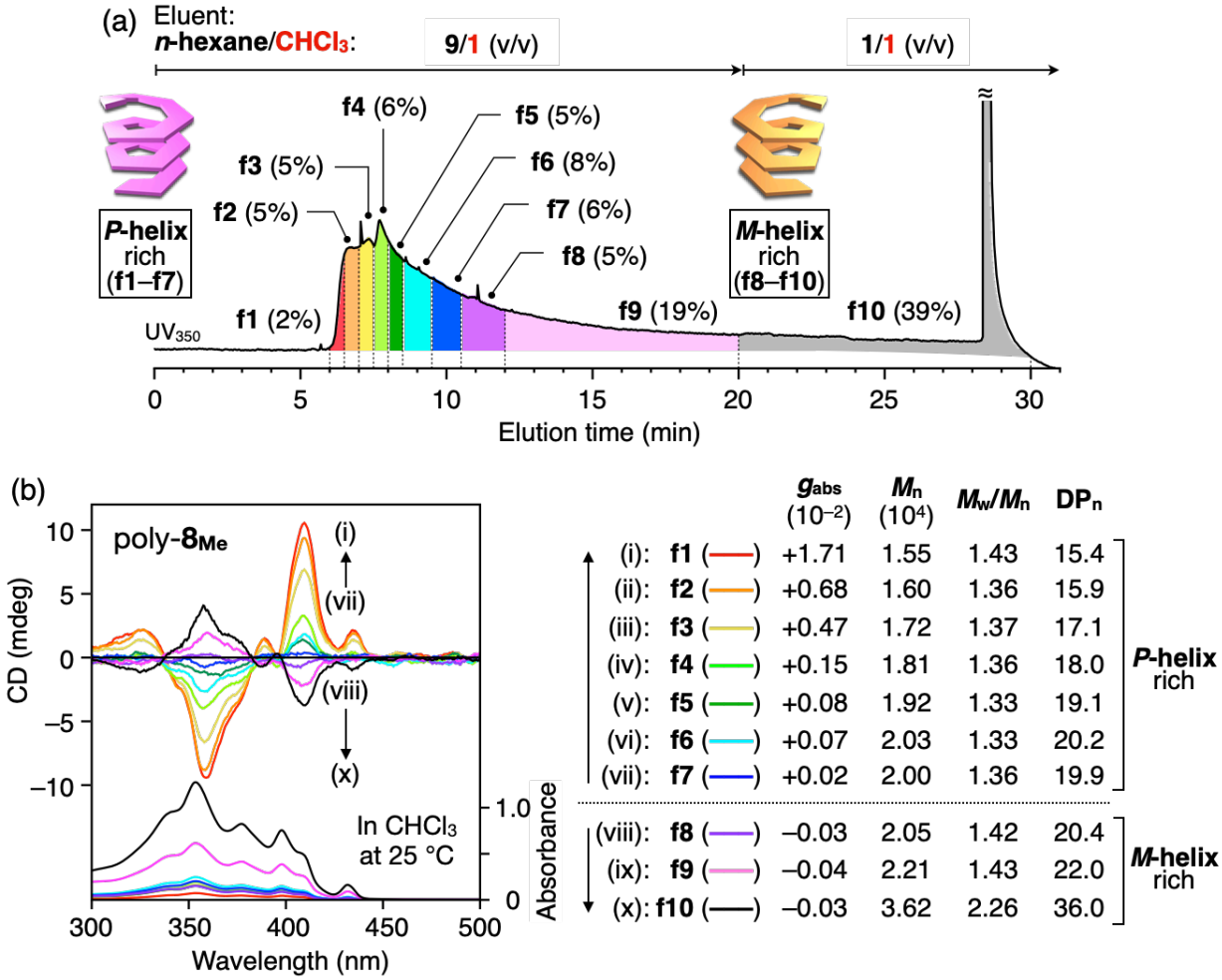

Figure 4. Chiral HPLC chromatogram of the as-synthesized poly-**8**$_{Me}$ under stepwise elution conditions. Chromatographic conditions: column, CHIRALPAK IG (2.0 cm (i.d.) × 25 cm); eluent, *n*-hexane/chloroform (9/1 (0 – 20 min) and 1/1 (>20 min), v/v); flow rate, 8.0 mL/min; temperature, 25 °C. (b) CD and absorption spectra of poly-**8**$_{Me}$ (**f1** – **f10**) obtained by chiral HPLC fractionation, measured in chloroform at 25 °C. Maximum Kuhn's dissymmetry *g*-factors at around 410 nm (g_{abs}) as well as the M_n, M_w/M_n, and DP_n values estimated by SEC (polystyrene standards) with chloroform as the eluent are also shown.

subjected to chiral HPLC on CHIRALPAK IG using *n*-hexane/chloroform (9/1, v/v) as the eluent at 25 °C, we observed a broad chromatographic peak with significant tailing (Figure S29a). Other more polar eluents, such as *n*-hexane/chloroform (1/1, v/v), resulted in mostly single sharp peaks with almost no retention (Figure S29b). With these elution profiles in mind, we employed the stepwise elution mode (*n*-hexane/chloroform = 9/1 to 1/1, v/v) at 25 °C with CHIRALPAK IG to fully recover the poly-**8**$_{Me}$ injected into the chiral HPLC system. The eluted peaks derived from poly-**8**$_{Me}$ were then fractionated into 10 fractions as shown in Figure 4a, in which the early-eluting components tended to have lower M_n values than the late-eluting ones in the range of 1.55×10^4 (**f1**) – 3.62×10^4 (**f10**) (Figure 4b) probably due to a relatively weak interaction between the low molar mass polymers and the chiral stationary phase. Interestingly, the former 1–7 (**f1**–**f7**) and latter 8–10 (**f8**–**f10**) fractions displayed mirror-image circular dichroism (CD) spectra in the π-conjugated polymer backbone chromophore regions (300 – 450 nm) (Figure 4b), providing conclusive evidence that the poly-**8**$_{Me}$ definitely exists as a pair of (*P*)- and (*M*)-handed helices stable in solution. To the best of our knowledge, this is the first example of the isolation of optically-active fully π-conjugated helical ladder polymers composed of entirely achiral monomer units showing an optical activity solely due to the macromolecular helicity.

Based on the time-dependent-density functional theory calculations of a (*P*)-handed helical oligomer model ((*P*)-model-**a**) (Figure S30), the helical sense of the poly-**8**$_{Me}$ (**f1**–**f7**) showing the positive and negative Cotton effect signs at 410 and 360 nm, respectively (Figure 4b(i–vii)), was assigned to the (*P*)-helix, and hence, the (*M*)-helix for the latter fractions (**f8**–**f10**) (Figure 4b(viii–x)). Although the helix-sense excess (*hse*) values of the fractionated poly-**8**$_{Me}$ samples remain unsolved, the Kuhn's dissymmetry factor (g_{abs}) of the fractionated poly-**8**$_{Me}$ (**f1**) reached 1.7×10^{-2} at a maximum (Figure 4b(i)), which is sufficiently high comparable to or exceeding those of the previously reported conjugated one-handed helical polymers, including polyisocyanides, polyisocyanates, polyacetylenes, and polysilanes,[23] as well as the partially conjugated one-handed helical ladder polymers (poly-**A**,[15] poly-**B**,[16] and poly-**C**[17]) (typically in the order of 10^{-3}). As a result, the *hse* value of the poly-**8**$_{Me}$ (**f1**) is presumed to be rather high (Figure 4b(i)).

The excess one-handed helical conformation of the isolated optically-active (*P*)-poly-**8**$_{Me}$ with the DP_n of more than 15 (a mixture of **f1**–**f3** fractions) was stable in 1,1,2,2-tetrachloroethane at 50 °C and maintained its optical activity for 24 h, indicating its relatively high helix-inversion barrier (Figure S31a,b). At higher temperatures (80 and 100 °C), the CD intensity of the (*P*)-poly-**8**$_{Me}$ tended to very slowly decrease with time due to inversion of

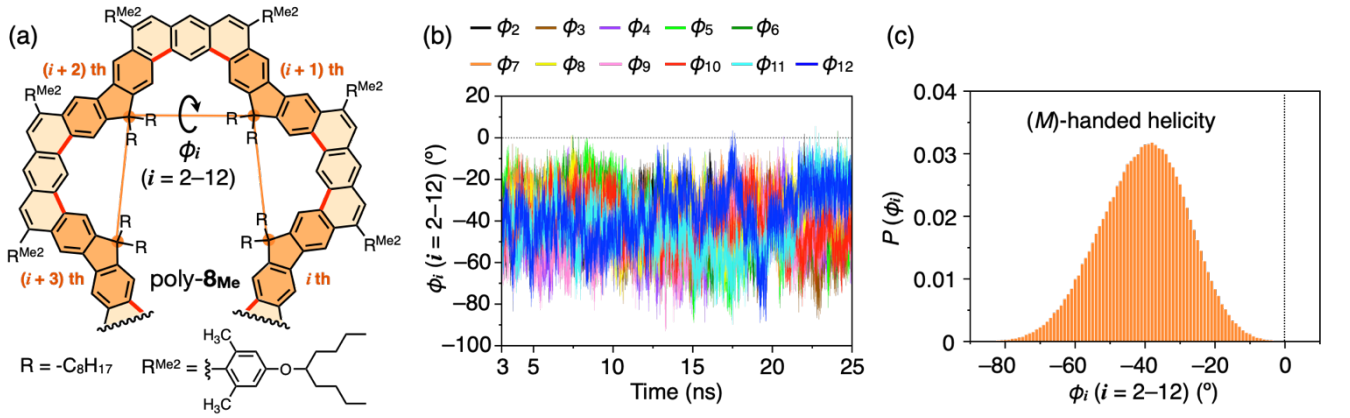

Figure 5. (a) Definition of the dihedral angle, ϕ_i (i = 2 – 12), among the sp^3 carbon atoms of the fluorene units in the i to (i + 3)th consecutive four repeating units (i = 2 – 12) of the poly-**8**$_{Me}$ model. (b) Plots of ϕ_i (i = 2 – 12) during the MD simulation at 323 K (50 °C). The ϕ_1 and ϕ_{13} at both terminals are excluded from the plot. (c) Probability distribution of ϕ_i (i = 2 – 12).

the helix-sense (racemization) (Figure S31a,c,d). Surprisingly, however, the CD intensity almost reached a plateau value after storage at 80 °C for 24 h, which remained unchanged for 4 days, but then gradually decreased at 100 °C. The observed unusual temperature-dependent stepwise racemization is probably attributed to the lower-molar-mass (*P*)-poly-**8**$_{Me}$ contained in the fractionated (*P*)-poly-**8**$_{Me}$, which would racemize faster than its higher-molar-mass one at higher temperatures.

We then synthesized a lower-molar-mass poly-**8**$_{Me}$ (M_n = 6.47 × 10^3; DP$_n$ = 6.4) with a narrow M_w/M_n of 1.25 (poly-**8**$_{Me}$-6.5K) (Scheme S4 and Figure S32a) from its precursor (poly-**7**$_{Me}$-7.1K) (Scheme S3 and Table S1) and performed the same chiral HPLC separation experiments (Figure S32a). However, the poly-**8**$_{Me}$-6.5K could not be resolved at all on the same chiral column and all the fractions showed no CD (Figure S32b). This is presumably because the poly-**8**$_{Me}$-6.5K's chain length is too short to form a thermodynamically-stable helical conformation in solution or its low helix-inversion barrier, therefore, no resolution or racemization occurred during the chiral HPLC.[24] These results reveal the dominant role of the chain length or DP$_n$ in stabilizing the single-handed helical conformation of the fully π-conjugated helical ladder polymers. The MD simulation of poly-**8**$_{Me}$ with 15 repeating units at 323 K (50 °C) showed that the dihedral angles (ϕ_i (i = 2 – 12) in Figure 5a) among the four consecutive repeating units of (*M*)-handed helical poly-**8**$_{Me}$ always have negative values, except for only a few instantaneous sign changes (Figure 5b),[25] indicating that each turn of the helix maintains its (*M*)-helicity during the simulation. Hence, the DP$_n$ of ca. 15, which corresponds to approximately 4 turns of the helix, is sufficient to obtain a thermodynamically-stable optically-active one-handed helical poly-**8**$_{Me}$.

In summary, we have succeeded in producing the first fully π-conjugated preferred-handed helical ladder polymer composed entirely of achiral monomer units through quantitative and chemoselective acid-promoted alkyne benzannulations of the rationally-designed random-coil precursor polymer by a combination of chromatographic enantioseparations. The macromolecular helicity was sufficiently stable in solution even at 100 °C due to the high helix-inversion barrier. We believe that the present results pave the way for the predictable synthesis of a variety of fully π-conjugated single-handed helical ladder polymers with the desired helical pitch and cavity size/geometry without embedding any precious chiral moieties, leading to the versatile and practical chiral materials for circularly polarized emitters, enantioselective encapsulations, chiral nanoreactors, and nanosolenoids. Work toward these goals is currently in progress in our laboratory and will be reported in due course.

Acknowledgements

This work was supported in part by JSPS KAKENHI (Grant-in-Aid for Specially Promoted Research, No. 18H05209 (E.Y. and T.I.) and Grant-in-Aid for Scientific Research (B), No. 21H01984 (T.I.)) and JST PRESTO (No. JPMJPR21A1 (T.I.)).

Keywords: defect-free synthesis • enantioseparation • fully π-conjugation • helical polymers • ladder formation

[1] For recent reviews, see: a) J. Lee, A. J. Kalin, T. Yuan, M. Al-Hashimi, L. Fang, *Chem. Sci.* **2017**, *8*, 2503–2521; b) Z. Cai, M. A. Awais, N. Zhang, L. Yu, *Chem* **2018**, *4*, 2538–2570; c) J. Chen, K. Yang, X. Zhou, X. Guo, *Chem. - Asian J.* **2018**, *13*, 2587–2600; d) Z. Cao, M. Leng, Y. Cao, X. Gu, L. Fang, *J. Polym. Sci.* **2022**, *60*, 298–310; e) K. Müllen, U. Scherf, *Macromol. Chem. Phys.* **2023**, *224*, 2200337.

[2] U. Scherf, K. Müllen, *Makromol. Chem., Rapid Commun.* **1991**, *12*, 489–497.

[3] a) A. C. Grimsdale, K. Müllen, *Macromol. Rapid Commun.* **2007**, *28*, 1676–1702; b) J. Chen, K. Yang, X. Zhou, X. Guo, *Chem. - Asian J.* **2018**, *13*, 2587–2600; c) A. V. Zasedatelev, A. V. Baranikov, D. Sannikov, D. Urbonas, F. Scafirimuto, V. Y. Shishkov, E. S. Andrianov, Y. E. Lozovik, U. Scherf, T. Stöferle, R. F. Mahrt, P. G. Lagoudakis, *Nature* **2021**, *597*, 493–497.

[4] a) A. Köhler, J. Grüner, R. H. Friend, K. Müllen, U. Scherf, *Chem. Phys. Lett.* **1995**, *243*, 456–461; b) M. M. Alam, S. A. Jenekhe, *Chem. Mater.* **2004**, *16*, 4647–4656; c) D. J. Lipomi, R. C. Chiechi, W. F. Reus, G. M. Whitesides, *Adv. Funct. Mater.* **2008**, *18*, 3469–3477; d) W. R. Hollingsworth, J. Lee, L. Fang, A. L. Ayzner, *ACS Energy Lett.* **2017**, *2*, 2096–2102; e) M. Grandl, J. Schepper, S. Maity, A. Peukert, E. von Hauff, F. Pammer, *Macromolecules* **2019**, *52*, 1013–1024.

[5] a) A. Babel, S. A. Jenekhe, *J. Am. Chem. Soc.* **2003**, *125*, 13656–13657; b) H. Usta, C. Risko, Z. M. Wang, H. Huang, M. K. Deliomeroglu, A. Zhukhovitskiy, A. Facchetti, T. J. Marks, *J. Am. Chem. Soc.* **2009**, *131*, 5586–5608; c) S. R. Bheemireddy, M. P. Hautzinger, T. Li, B. Lee, K. N. Plunkett, *J. Am. Chem. Soc.* **2017**, *139*, 5801–5807; d) A. V. Zasedatelev, A. V. Baranikov, D. Urbonas, F. Scafirimuto, U. Scherf, T. Stöferle, R. F. Mahrt, P. G. Lagoudakis, *Nat. Photonics* **2019**, *13*, 378–383; e) H. Y. Wu, C. Y. Yang, Q. Li, N. B. Kolhe, X. Strakosas, M. A. Stoeckel, Z. Wu, W. Jin, M. Savvakis, R. Kroon, D. Tu, H. Y. Woo, M. Berggren, S. A. Jenekhe, S. Fabiano, *Adv. Mater.* **2022**, *34*, 2106235.

[6] a) G. Grem, G. Leising, *Synth. Met.* **1993**, *57*, 4105–4110; b) U. Scherf, *J. Mater. Chem.* **1999**, *9*, 1853–1864; c) J. Jacob, S. Sax, T. Piok, E. J. W. List, A. C. Grimsdale, K. Müllen, *J. Am. Chem. Soc.* **2004**, *126*, 6987–6995; d) Y. Wu, J. Zhang, Z. Fei, Z. Bo, *J. Am. Chem. Soc.* **2008**, *130*, 7192–7193; e) E. Khodabakhshi, C. Ramanan, J. J. Michels, S. Bonus, D. Hertel, K. Meerholz, M. Forster, U. Scherf, P. W. M. Blom, *Adv. Electron. Mater.* **2020**, *6*, 2000082.

[7] a) J. Wu, X. Rui, G. Long, W. Chen, Q. Yan, Q. Zhang, *Angew. Chem., Int. Ed.* **2015**, *54*, 7354–7358; b) J. Xie, Q. Zhang, *J. Mater. Chem. A* **2016**, *4*, 7091–7106; c) Y. Chen, H. Li, M. Tang, S. Zhuo, Y. Wu, E. Wang, S. Wang, C. Wang, W. Hu, *J. Mater. Chem. A* **2019**, *7*, 20891–20898; d) R. R. Kapaev, A. F. Shestakov, S. G. Vasil'ev, K. J. Stevenson, *ACS Appl. Energy Mater.* **2021**, *4*, 10423–10427.

[8] a) J. Li, X. Wan, *J. Polym. Sci., Part A: Polym. Chem.* **2013**, *51*, 4694–4701; b) K. Yu, X. Ji, T. Yuan, Y. Cheng, J. Li, X. Hu, Z. Liu, X. Zhou, L. Fang, *Adv. Mater.* **2021**, *33*, 2104558.

[9] a) K. Xu, H. Sun, T.-P. Ruoko, G. Wang, R. Kroon, N. B. Kolhe, Y. Puttisong, X. Liu, D. Fazzi, K. Shibata, C.-Y. Yang, N. Sun, G. Persson, A. B. Yankovich, E. Olsson, H. Yoshida, W. M. Chen, M. Fahlman, M. Kemerink, S. A. Jenekhe, C. Müller, M. Berggren, S. Fabiano, *Nat. Mater.* **2020**, *19*, 738–744; b) T. L. D. Tam, M. Lin, S. W. Chien, J. Xu, *ACS Macro Lett.* **2022**, *11*, 110–115.

[10] a) W. A. Chalifoux, W. Yang, *Synlett* **2017**, *28*, 625–632; b) Y. C. Teo, H. W. H. Lai, Y. Xia, *Chem. - Eur. J.* **2017**, *23*, 14101–14112; c) X. Y. Wang, A. Narita, K. Müllen, *Nat. Rev. Chem.* **2018**, *2*, 0100; d) C. Z. Zhu, A. J. Kalin, L. Fang, *Acc. Chem. Res.* **2019**, *52*, 1089–1100; e) W. Chen, F. Yu, Q. Xu, G. Zhou, Q. Zhang, *Adv. Sci.* **2020**, *7*, 1903766; f) A. Jolly, D. D. Miao, M. Daigle, J.-F. Morin, *Angew. Chem., Int. Ed.* **2020**, *59*, 4624–4633; g) Z.-D. Yu, Y. Lu, J.-Y. Wang, J. Pei, *Chem. - Eur. J.* **2020**, *26*, 16194–16205.

[11] a) M. Daigle, D. Miao, A. Lucotti, M. Tommasini, J.-F. Morin, *Angew. Chem., Int. Ed.* **2017**, *56*, 6213–6217; b) M. Daigle, J.-F. Morin, *Macromolecules* **2017**, *50*, 9257–9264; c) K. M. Magiera, V. Aryal, W. A. Chalifoux, *Org. Biomol. Chem.* **2020**, *18*, 2372–2386; d) D. D. Miao, V. Di Michele, F. Gagnon, C. Aumaître, A. Lucotti, M. Del Zoppo, F. Lirette, M. Tommasini, J.-F. Morin, *J. Am. Chem. Soc.* **2021**, *143*, 11302–11308; e) J. Wang, Y. Zhu, G. Zhuang, Y. Wu, S. Wang, P. Huang, G. Sheng, M. Chen, S. Yang, T. Greber, P. Du, *Nat. Commun.* **2022**, *13*, 1239.

[12] Z. P. Liu, Y. D. Guo, X. H. Yan, H. L. Zeng, X. Y. Mou, Z. R. Wang, J. J. Wang, *J. Appl. Phys.* **2019**, *126*, 144303.

[13] T. Iwasaki, Y. Kohinata, H. Nishide, *Org. Lett.* **2005**, *7*, 755–758.

[14] X. Xiao, Q. Cheng, S. T. Bao, Z. Jin, S. Sun, H. Jiang, M. L. Steigerwald, C. Nuckolls, *J. Am. Chem. Soc.* **2022**, *144*, 20214–20220.

[15] T. Ikai, T. Yoshida, K.-i. Shinohara, T. Taniguchi, Y. Wada, T. M. Swager, *J. Am. Chem. Soc.* **2019**, *141*, 4696–4703.

[16] W. Zheng, K. Oki, R. Saha, Y. Hijikata, E. Yashima, T. Ikai, *Angew. Chem., Int. Ed.* **2023**, *62*, e202218297.

[17] W. Zheng, T. Ikai, E. Yashima, *Angew. Chem., Int. Ed.* **2021**, *60*, 11294–11299.

[18] a) M. B. Goldfinger, T. M. Swager, *J. Am. Chem. Soc.* **1994**, *116*, 7895–7896; b) M. B. Goldfinger, K. B. Crawford, T. M. Swager, *J. Am. Chem. Soc.* **1997**, *119*, 4578–4593.

[19] T. Ikai, S. Yamakawa, N. Suzuki, E. Yashima, *Chem. - Asian J.* **2021**, *16*, 769–774.

[20] Very recently, Schneebeli and coworkers reported an experimental and computational study on a similar springlike extension/contraction motion of partially conjugated helical ladder polymers composed of chiral repeating units, see: K. E. Murphy, K. T. McKay, M. Schenkelberg, M. Sharafi, O. Vestrheim, M. Ivancic, J. Li, S. T. Schneebeli, *Angew. Chem., Int. Ed.* **2022**, *61*, e202209772.

[21] For splitting of aromatic proton resonances of ladder polymers caused by hindered rotation of alkyl chains, see: a) J. Lee, B. B. Rajeeva, T. Yuan, Z.-H. Guo, Y.-H. Lin, M. Al-Hashimi, Y. Zheng, L. Fang, *Chem. Sci.* **2016**, *7*, 881–889; b) J. Lee, A. J. Kalin, C. Wang, J. T. Early, M. Al-Hashimi, L. Fang, *Polym. Chem.* **2018**, *9*, 1603–1609.

[22] a) R. J. M. Nolte, A. J. M. Van Beijnen, W. Drenth, *J. Am. Chem. Soc.* **1974**, *96*, 5932–5933; b) Y. Okamoto, H. Mohri, T. Nakano, K. Hatada, *J. Am. Chem. Soc.* **1989**, *111*, 5952–5954; c) T. Sakamoto, Y. Fukuda, S.-i. Sato, T. Nakano, *Angew. Chem., Int. Ed.* **2009**, *48*, 9308–9311; d) T. Miyabe, H. Iida, M. Banno, T. Yamaguchi, E. Yashima, *Macromolecules* **2011**, *44*, 8687–8692; e) T. Ikai, S. Kawabata, F. Mamiya, D. Taura, N. Ousaka, E. Yashima, *J. Am. Chem. Soc.* **2020**, *142*, 21913–21925.

[23] a) M. M. Green, J. W. Park, T. Sato, A. Teramoto, S. Lifson, R. L. B. Selinger, J. V. Selinger, *Angew. Chem., Int. Ed.* **1999**, *38*, 3139–3154; b) M. Fujiki, *Macromol. Rapid Commun.* **2001**, *22*, 539–563; c) E. Yashima, K. Maeda, H. Iida, Y. Furusho, K. Nagai, *Chem. Rev.* **2009**, *109*, 6102–6211; d) E. Yashima, N. Ousaka, D. Taura, K. Shimomura, T. Ikai, K. Maeda, *Chem. Rev.* **2016**, *116*, 13752–13990.

[24] For molar mass-dependent stability of a one-handed helical conformation of helical polymers, see: a) J. C. Nelson, J. G. Saven, J. S. Moore, P. G. Wolynes, *Science* **1997**, *277*, 1793–1796 ; b) K. Maeda, K. Morino, Y. Okamoto, T. Sato, E. Yashima, *J. Am. Chem. Soc.* **2004**, *126*, 4329–4342; c) H. Jiang, V. Maurizot, I. Huc, *Tetrahedron* **2004**, *60*, 10029–10038; d) Y. Nagata, T. Nishikawa, M. Suginome, *J. Am. Chem. Soc.* **2014**, *136*, 15901–15904; e) K. Maeda, M. Nozaki, K. Hashimoto, K. Shimomura, D. Hirose, T. Nishimura, G. Watanabe, E. Yashima, *J. Am. Chem. Soc.* **2020**, *142*, 7668–7682.

[25] The instantaneous sign change of one of the dihedral angles (ϕ) would not cause the helicity inversion, because the changed sign reverted back to the original one immediately.